Aging distorts the representation of emotions by amplifying prefrontal variability

Gargi Majumdar[1], Fahd Yazin[1,2], Arpan Banerjee[1*], Dipanjan Roy[1,3*]

1 Cognitive Brain Dynamics Lab, National Brain Research Centre, NH-8, Manesar, Gurugram, 122052, India.

2 The University of Edinburgh 57 George Square Edinburgh EH8 9JU

3 Center for Brain Science and Applications (CBSA), School of AIDE, Indian Institute of Technology, Jodhpur 342030, India.

* Corresponding authors

Email: arpan@nbrc.ac.in (Dr Arpan Banerjee); droy@iitj.ac.in (Dr Dipanjan Roy)

Abstract

Effectively navigating a complex social life requires stable representations of emotions, thereby necessitating an optimal computation of uncertainty around it. Here, we focus on a regime where this optimal estimation of uncertainty is disrupted – healthy aging and its consequences on their emotional experiences. Our findings indicate that older adults represent an increased uncertainty around emotions, leading to variable emotional response profiles across a range of emotional tasks. Furthermore, the boundaries between emotional categories become less distinct with age, causing substantial overlap between adjacent emotions compared to younger individuals. By employing a Bayesian learning model, we revealed that these age-related effects emerge from an increased predictive uncertainty of emotional valence during hierarchical inference. Crucially, model outputs were consistent with neural signatures in the lateral orbitofrontal cortex across young and older brains while watching an emotionally intense movie. Specifically, we found that older adults exhibit heightened neural variability in this region with distorted latent dynamics, contributing to their overall variable emotional experience. Taken together, we aimed to integrate disparate evidence in age-associated emotional changes under a unified framework of misestimation of uncertainty.

Significance Statement

With an increase in average lifespan, older individuals will be required to take greater responsibility for their physical and emotional wellbeing. However, the nature and neural underpinnings of age-associated emotional changes still remain a paradox. Without a well-grounded theoretical principle, the neurocognitive theories that ensued to explain these alterations have yielded significant inconsistencies especially in relation to emotion processing under naturalistic real-world scenarios. Combining evidence from large-scale behavioral and neuroimaging data on both simple and naturalistic emotional tasks, we demonstrated that these idiosyncratic emotional responses with aging, stems from their suboptimal computation of uncertainty during hierarchical inference, manifested as increased neural variability and distorted latent state representations in lateral orbitofrontal cortex. Together, our findings illustrate that age-associated emotional changes can be unified under a singular framework of misestimation of uncertainty, within a Bayesian brain purview, without the need for bespoke theories to explain disjunctive evidence.

Introduction

Similar experiences often elicit variable emotional responses. Bayesian brain frameworks offer an attractive and principled way to formalize this variability as a probabilistic inference (DC Knill, 2004). By estimating the uncertainty around the expected outcome, we can effectively account for this variability for both perceptual and higher-order cognitive processes (Clark, 2013). However, having a high uncertainty around one's emotional hypothesis might not be optimal as it entails inconsistency in one's experience, setting up harmful tension between opposing emotions, even to the same stimuli, leading to varying responses. Such idiosyncrasy has been pervasively observed in the emotional responses of healthy aging population (Campbell et al., 2015; Visser, 2020) but remains largely unexplored. While existing psychological theories like Socioemotional Selectivty theory (SST), Dynamic Integartion Theory (DIT), Stength and Vulnerability Integartion Theory (SAVI), and the positivity effect (Reed & Carstensen, 2012) have delved into the emotional shifts of the elderly, their explanation remains often confined to specific paradigms, leading to inconsistencies with introduction of complex stimuli (Atkinson et al., 2021; Cortes et al., 2021; Schweizer et al., 2019). Moreover, these theories lack a robust computational architecture, posing a challenge to bridge the gap between knowledge articulated at different levels (neural to behavioral) of analysis.

Here we test an alternative theory - aging introduces a significant variability around the valence, reflecting a misrepresentation of uncertainty (Nassar et al., 2016) in inferred emotions. This can manifest as idiosyncratic responses on the group level but often has deeper, statistical changes within an individual behaviourally and neurally that stem from a diffuse, highly overlapping representation of emotions. Consider the classic circumplex model of emotions (Fig. 1) (Posner et al., 2005) which assumes the organization of different emotional categories on an arousal-valence plane. This suggests individuals represent emotions putatively as organized according to two dimensions. However, increased variability around an emotion not only would compromise this ability but also result in a systematic ‘spill-over’ of adjacent emotions (but not distant ones) into each other, contributing to a highly variable emotional profile, that may have signatures in cortical regions involved.

Neural variability is an attractive and logical consequence of stimulus variability, with strong computational foundations demonstrating how the latter can modulate the former in perceptual studies (Hénaff et al., 2020, Festa et al., 2021). Moreover, an important line of study in healthy aging involves

investigating cognitive flexibility in tasks. Specifically, an optimal response to uncertainty in the environment can materialize through an optimally higher neural variability (Garrett et al.,2017). However, different subregions and networks can tackle different aspects of any given task, thereby making whole-brain approaches less informative. Prior research has demonstrated that the lateral orbitofrontal cortex (lOFC) is responsible for continuously tracking the evolving uncertainty in an affective setting, with its latent state dynamics closely aligning with how a Bayesian learner would temporally estimate uncertainty (Majumdar et al., 2023). Parallelly, recent studies have shown that poorer performance of the older adults in dynamic decision-making tasks is characterised by a misestimation of uncertainty (Bruckner et al., 2020; Nassar et al., 2016). Combining these sets of burgeoning evidence, we extend our hypothesis neurally by proposing that the behavioral variability around the valence, would be associated with and probably mediated by an increased variability in lOFC, which would be a signature of affective dynamics in aging. Thus, our central hypothesis posits that misestimation of uncertainty leads to a misrepresentation of emotions in the elderly brains.

In order to test this out, we first assessed emotional responses from the two age groups from a family of emotional tasks – facial emotion recognition, discrete ratings of small video clips and continuous ratings from a naturalistic movie. Next, we constructed and contrasted multiple variants of a Bayes optimal (predictive) learning model, motivated by specific predictions of miscomputation of uncertainty in the elderly during affective experience, to account for their idiosyncratic responses. A normative variant of this had previously enabled us to naturally estimate the uncertainty arising from the continuous valence time-course in the younger group. Here, we investigated whether older people differed with regards to computation of variance around the valence. This was examined on both the behavioural and neural data with an emphasis on lOFC which showed increased neural variability with a distinct change in its latent dynamics, and temporal representations with age. Together, we aimed to provide a parsimonious explanation for several apparently contradictory results in the emotion-aging literature under a singular framework of misrepresentation and miscomputation of uncertainty.

Result

Behavioural idiosyncrasy of older adults in emotional tasks

To robustly capture the age-associated changes in affective processing, we exploited three different datasets (Majumdar et al., 2023; Taylor et al., 2017), including both discrete and naturalistic emotional tasks (See Materials and Methods).

Increased variability of older individuals to facial emotions

Young (N = 108, 18-35 years) and older (N = 95, 60-88 years) adults had to report the displayed emotion on a morphed image of a facial expression (FER) from 6 emotion categories – Happy, Sad, Anger, Fear, Disgust and Surprise. In accordance with previous findings, we found a significantly reduced accuracy in old for all emotion categories (Happy: $t = 3.54$, $p < 0.001$, Cohen's $d = 0.5$; Sad: $t = 7.01$, $p < 0.0001$, $d = 0.99$; Anger: $t = 4.54$, $p < 0.0001$, $d = 0.6$; Fear: $t = 8.06$, $p < 0.0001$, $d = 1.13$; Surprise: $t = 6.61$, $p < 0.0001$, $d = 0.9$) except disgust ($p = 0.2$) (Fig. 1b). This difference was more pronounced for negative emotions, with the highest in Fear and the least in Happy.

Next, to obtain a more nuanced understanding of their profile of responses, we computed a co-occurrence matrix of the true emotion (of a face) and the responded emotion by the participants, for each group. For example, if, out of 100 instances of Fear trials, 80 accurate Fear responses were paired with 20 inaccurate Surprise responses, we could infer that Surprise had a 'spill-over' effect into the Fear category. For visualization, we collapsed it across participants for all six emotion categories for each group (values adjusted based on a predetermined threshold). Fig. 1c shows that older individuals exhibited substantial bidirectional overlap between surprise and fear indicating significant overlapping representation of these two emotions. Similar patterns are observed between anger and disgust, as well as between anger and fear. Notably, these emotions are adjacently placed in the circumplex model. If the observed overlap were solely a result of their variability in representing faces, one would expect equal overlap among all emotions, which is not the case. Likewise, this phenomenon cannot be purely attributed to the variability in representing negative emotions in general, as it fails to explain the specificity observed between adjacent emotions (e.g. no overlap between anger and sadness, placed much distantly than disgust or fear). Crucially, young adults showed significant overlap only between fear and surprise.

This led us to investigate whether the observed emotion overlaps in older individuals is linked in their increased individual variability in emotional responses. We compared the individual variability of the participants by computing the standard deviation (SD) of their accuracy over all 6 categories and found a significantly higher SD in old (mean-SD_Y = 11.08, mean-SD_O = 17.44, t = -5.17, p < 0.0001, Cohen's d = 17.44) (Fig. 1d). Interestingly, between-group variability for each of the 6 categories showed a similar pattern of increased idiosyncrasy in older adults (Happy: SD_Y = 2.68, SD_O = 5.99; Sad: SD_Y = 5.02, SD_O = 19.31; Anger: SD_Y = 19.52, SD_O = 27.4; Fear: SD_Y = 15.4, SD_O = 23.54; Disgust: SD_Y = 20.28, SD_O = 20.63; Surprise: SD_Y = 8.04, SD_O = 13.32) (Fig. S1, SI Appendix).

Increased variability of older adults to complex dynamic emotions

The above result suggests age-associated variability around valence is plausible for increased variability in emotion perception. An alternate explanation for this could be variable encoding of specific face-emotion links. Thus, we sought to test out our prediction on increased idiosyncrasy in old in a more naturalistic set-up. Here, participants had to rate (0-100) small video clips (~30s) of Neutral, Negative and Positive valence on how negative and positive they felt while watching the clip. No significant difference was observed between the negatively-rated negative clips (NegW_neg: t = -0.5, p = 0.32) and positively-rated positive clips (PosW_pos: t = -0.5, p = 0.31) between the Young (N = 49, μ_{age} = 28 yrs) and Old (N = 42, μ_{age} = 76yrs) (Fig. 1e). However the other four conditions showed significant difference between the two groups with older people showing higher positive and negative ratings (NegW_pos: t = -6.8, p<0.0001; PosW_neg: t = -4.9, p<0.0001; NeuW_neg: t = -8, -p<0.0001; NeuW_pos: t = -6.4, p<0.0001) for all conditions. These conditions require one to shift one's felt affect across various emotional polarities. That is, requiring one to experience a specific tone of emotion (e.g. negative) and report how positive it was, showed significant differences between the groups. This further strengthened our motivation to investigate the emotional variability in the elderly to determine if they exhibit more consistent evidence, contrary to the positivity bias. For this, we calculated the between-group SD of their ratings for each condition. All 6 conditions showed a consistent increase in variability in old irrespective of the valence (NegW_pos: SD_Y = 0.47, SD_O = 1.75, NegW_neg: SD_Y = 1.38, SD_O = 2.43; PosW_pos: SD_Y = 1.90, SD_O = 2.36; PosW_neg: SD_Y = 0.74, SD_O = 1.47; NeuW_pos: SD_Y = 1.18, SD_O = 2.29; NeuW_neg: SD_Y = 0.40, SD_O = 1.42) (Fig. 1f).

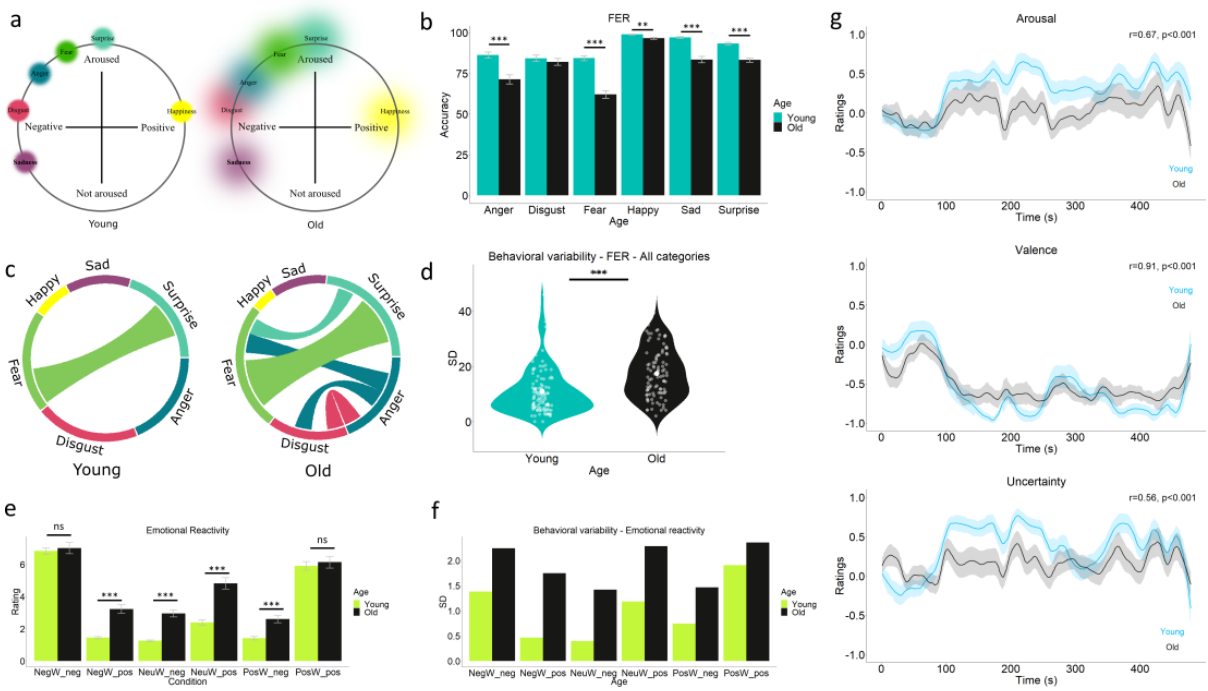

Figure 1*: Graphical illustration of our hypothesis and behavioral results. (a) Our main hypothesis posited that decreased precision or increased variance (represented as coloured circles around emotion categories) around the valence leads to the misrepresentation of emotions in older adults. (b) Behavioral accuracy of Facial Emotion Recognition (FER) task shows mean accuracy of the older adults were significantly lower than young for all categories (p<0.001) except Disgust (p=0.2). (c) Chord diagram showing a "spill-over" effect of adjacent categories in older adults. (d) In the FER task, individual variability, computed as the standard deviation (SD) of each participant's accuracy over all 6 categories depicts significantly higher behavioral variability in older adults compared to young (mean-*SD_{Young} *= 11.08, mean-*SD_{Old} *= 17.44, P<0.0001). (e) Subjective ratings for the Emotional Reactivity (EmoR) task in both groups display no significant difference in the ratings between the two groups for negatively-rated-negative (NegW_neg) clips and positively-rated-positive clips (PosW_pos) (NegW_neg: p = 0.32; PosW_pos: p = 0.31). (f) Between-group SD of the EmoR ratings shows increased variability in behavioral responses in the old compared to young for all conditions. (g) Continuous ratings of Arousal, Valence and Uncertainty of both groups for the movie "Bang!You're dead". (top) Older adults exhibit lower arousal than (r=0.67, p<0.001). (middle) Both groups indicate a strong correlation for the valence ratings (r=0.91, p<0.001). (bottom) Uncertainty ratings show the least correlation (r=0.56, p<0.001) between the two groups with more frequent fluctuations in the elderly.*

Increased variability of older individuals in ongoing predictions in emotional movie-watching task

The above results suggest that age-associated bias towards positive emotion disappears with the introduction of naturalistic paradigms (Cortes et al., 2021), but their idiosyncratic responses persist possibly due to the observed "spill-over" effects of different emotion categories. This also entails that navigating through the emotional landscape pronounces the differences in emotional experience in older adults.

However a single scalar rating of a movie can hide the evolving temporal dimensions of emotions (emotion dynamics), or the affective trajectory one takes (Majumdar et al., 2023). These offer a glimpse into the precise dynamics underlying their idiosyncratic response. For this, we proceeded to conduct an online experiment to collect continuous ratings of Arousal (Y = 17; O = 15), Valence (Y = 17; O =15) and Uncertainty (Y = 16; O =17) on the movie “Bang! You’re dead” (8mins) (same stimulus as that of the neuroimaging participants) from 6 independent groups of young and older adults (SI Appendix, Table S1). An overall lower and variable arousal in the elderly ($r = 0.67$, $p < 0.001$) suggested their less intense emotional experience of the movie compared to the young. However, both the groups appeared to perceive the valence very similarly ($r = 0.91$, $p < 0.001$) (Fig. 1g). Interestingly, the uncertainty ratings (which denotes the uncertainty around the expected outcome, thereby dependent on the valence of the expected outcome), showed the weakest correlation ($r = 0.56$, $p < 0.001$) of the three affective dimensions, with frequent fluctuations in the old. An increased variability around the valence would be manifested by an increase in this uncertainty, which is why we chose this measure.

To further examine whether this pattern is also evident at the neural level, we constructed a Bayesian Hierarchical Regression (BHR) model to discern the effect of valence and uncertainty in modulating the neural activity between the two groups (SI Appendix, Fig. S1) for emotionally intense scenes. The model architecture taking into account different scenes and individual variability strongly builds on our previous validation study (Majumdar et al., 2023). To address the critique on the objectivity of scene-classification from young’s ratings, we performed all our main analyses on the entire movie. Posterior density estimates of the BHR showed that the effect of uncertainty is significantly different between the two groups (Young: $P = 0.98$, 95% HDI = [0.005, 0.11]; Old: $P = 0.98$, 95% HDI = [-0.1, -0.006]) compared to the valence (Young: $P = 0.77$, 95% HDI = [-0.05, 0.09]; Old: $P = 0.64$, 95% HDI = [-0.07, 0.05]). Additionally, to control for the role of attention in older individuals we performed an engagement analysis (SI Appendix, Fig. S2), which showed emotional scenes followed a similar engagement pattern in both groups.

Convergent evidence from both behavioral and neural level thus far indicated an increased variability of emotional experiences in the old, with a significant difference in the perception of uncertainty around the valence of expected outcome (rather than valence) with age. Can these idiosyncratic responses be stemming from an age-associated misestimation of uncertainty during affective experience?

Misestimation of uncertainty during affective experience in old

To identify the specific computational alterations that might be driving the differences in uncertainty estimation across healthy aging during affective experience, we deployed multiple 3-layered Hierarchical Gaussian Filter (HGF) models (See Materials and Methods, SI Appendix) (Fig. 2a), each representing specific hypothesis. Here, we wanted to dynamically model the averaged valence rating of the elderly, by lesioning 2 free parameters - $\boldsymbol{\omega}$ and $\boldsymbol{\vartheta}$, which influences the estimated uncertainty (second-level) and volatility (third-level) trajectories about the valence respectively. A reduced $\boldsymbol{\omega}$ in the older adults would suggest a decreased prediction uncertainty around the valence dynamics, whereas an increased $\boldsymbol{\omega}$ will signify increased variance around the predictions of valence, independent of the volatility trajectory. The meta-volatility parameter $\boldsymbol{\vartheta}$, on the 3rd level determines the belief about the model's volatility of valence.

Model inversion was conducted by variational inference, and model adjudication was done by selecting the one with the highest log-model evidence (LME) (SI Appendix, TableS2). A central pattern emerged from the model. An increased $\boldsymbol{\omega}$ (Fig. 2b) suggested an increased variance (uncertainty) around the valence in the elderly. As a consequence, we observed higher variance of the belief trajectory of uncertainty (sa2) around the valence in old compared to young (Fig. 2c). This can explain the primary trend in the behavioural results – increased variability in estimating the valence with overlapping emotion representations and consequently the idiosyncratic responses in tasks and in movies.

Unstable latent state transitions in the OFC reflect the misrepresentation of uncertainty in old

The above results offered evidence to our hypothesis that, there is a considerable variance around the valence in the older adults in concordance with the variability of responses observed in the behavioral tasks. A consequence of this from the model is that owing to high variability, rapid updates to predictions are observed in older adults' ratings. Given the role of the lOFC in encoding uncertainty during affective experiences, particularly exhibited by its most abstract representation of the uncertainty at the neural level, we can postulate that changes in predictions would also be rapid in this region for the elderly, which would manifest in the neural latent state transitions. For this, we first performed a multivariate Hidden Markov Model (HMM) on the BOLD timeseries of each participant for the two groups as an

independent sequence to uncover the hidden states (See Materials and Methods). Model adjudication was done by selecting the one with the least BIC. In young adults, the lOFC showed 5 distinct states with mostly synchronous state transitions with their belief update trajectories obtained from the HGF (Fig. 2d - top). However, in the older adults, lOFC showed 3 states with frequent transitions with much faster belief updates (Fig. 2d - bottom) as a consequence of increased variance around the valence.

Thus both the prediction dynamics (from the model) and neural dynamics (from the HMM) displayed a common feature – that in older individuals, an increased variability around valence is reflected in how fast the internal dynamics change, possibly carrying with them the signatures of predictions and thus the affective dynamics.

We also compared the HMM state transitions of the VC as a control ROI for the two groups (Fig, S3), to eliminate any concern regarding the sensory perceptual differences. Both groups exhibited faster transitions with no distinct pattern.

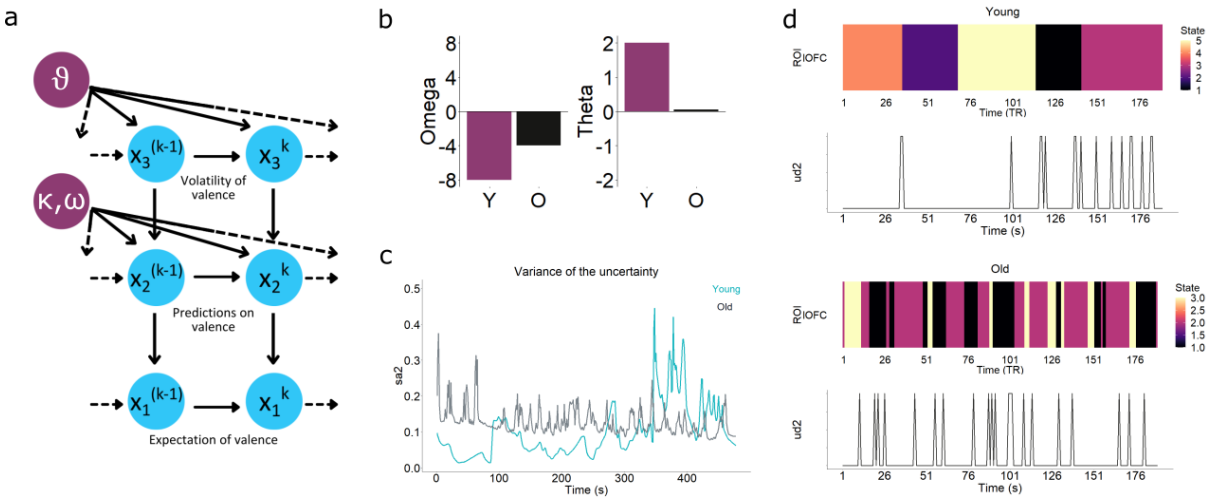

Figure 2: *Misestimation of uncertainty stemming from miscomputation of uncertainty (a) Graphical illustration of the HGF. x_1 represents beliefs about the changing valence, which in turn is affected by x_2, representing the belief on the predictions of valence. x_3 estimates the model volatility related to the valence timecourse, which in turn affects x_2. The levels are coupled via a phasic, time-varying parameter kappa (k). A tonic, time-invariant parameter omega (**ω**) influences the variance of the Gaussian walk at x_2, while theta (**ϑ**) determines the variance of the volatility. (b) Parameter comparisons between the age group show an increased **ω** and reduced **ϑ** in the elderly. (c) Higher **ω** leads to increased variance (sa2) associated with the predictions on the valence (x_2) in the elderly. (d) lOFC state transitions are specific to ongoing belief updates in young (top). Older adults show much frequent state transitions in lOFC and manifested as faster updates of their belief on the predictions of valence.*

Increased neural variability in the OFC is related to emotional variability in older adults

The above results established a link between the increased variability around the valence at the computational level and the frequent latent state transitions in lOFC, possibly reflecting the rapid prediction updates in the elderly. Could this be further linked to an intrinsic neural variability within this region while processing dynamic affect in the elderly?

Our model of the behavioral ratings offered insights into this question. The research on neural variability has gained significant momentum in aging studies, particularly in resting states, as it can serve as a predictor of behavioral flexibility. Thus, to discern whether this variability is a trait or solely induced by the affective states of movies, we need to the analyse both rest and movie scenarios. To address this, we integrated all prefrontal cortex (PFC) regions, visual cortex and PCC (a major hub of the Default Mode Network) in both resting and movie-watching states within a Bayesian hierarchical regression model. To quantify the variability, we computed the SD on the extracted BOLD of all ROIs for both conditions. Next, to delineate the effect of rest and movie with age on neural variability of these ROIs, we constructed a BHR with the SD_{BOLD} as independent variables. Firstly, this allowed us to assess whether the BOLD variability associated with these regions, is driven primarily by structural changes with age in which case SD_{BOLD} would be significantly different between the two groups for both conditions. However, we observed a significant increase in the SD_{BOLD} for the older individuals for the movie and not the rest (Movie: P = 0.99, BF >100; Rest: P = 0.84, BF = 5.84) (Fig. 3b).

Secondly, it also allowed us to identify the specific regions whose variability is significantly affected in both conditions with age. Interestingly the movie significantly affected the SD_{BOLD} of both lOFC (β_{mean} = 0.17, 95% HDI = [0.12, 0.23], P = 0.99) and mOFC (β_{mean} = -0.05, 95% HDI = [-0.1, 0.0004], P = 0.97) in the elderly and not the young (lOFC: β_{mean} = 0.031, 95% HDI = [-0.017, 0.085], P = 0.92; mOFC: β_{mean} = -0.005, 95% HDI = [-0.05, 0.05], P = 0.55) (Fig. 3c). No ROI showed significant increase in neural variability as an effect of the movie in young.

In rest, significant neural variability was only observed in ACC (β_{mean} = 0.075, 95% HDI = [0.020, 0.13], P = 0.99) and dlPFC (β_{mean} = -0.083, 95% HDI = [-0.14, -0.029], P = 0.99) but not the other prefrontal areas lOFC (β_{mean} = 0.014, 95% HDI = [-0.043, 0.07], P = 0.71), mOFC (β_{mean} = -0.0334, 95% HDI = [-0.089, 0.024], P = 0.88), vlPFC (β_{mean} = 0.055, 95% HDI = [-0.0016, 0.11], P = 0.97), mPFC (β_{mean} = 0.034, 95% HDI = [-0.017, 0.095], P = 0.92), dmPFC (β_{mean} = -0.018, 95% HDI = [-0.076, 0.036], P = 0.78) (Fig. 3d) in old. For the young, the resting state significantly affected the neural variability only in

lOFC (β_{mean} = 0.10, 95% HDI = [0.04, 0.17], P = 0.99) and dlPFC (β_{mean} = -0.12, 95% HDI = [-0.19, -0.05], P = 0.99), and not the other prefrontal areas (mOFC (β_{mean} = -0.005, 95% HDI = [-0.07, 0.06], P = 0.54), vlPFC (β_{mean} = 0.02, 95% HDI = [-0.05, 0.08], P = 0.65), mPFC (β_{mean} = 0.018, 95% HDI = [-0.05, 0.087], P = 0.75), dmPFC (β_{mean} = -0.033, 95% HDI = [-0.10, 0.034], P = 0.86), ACC (β_{mean} = 0.047, 95% HDI = [-0.022, 0.11], P = 0.92)) (Fig. 3d). This suggested that the neural variability of lOFC undergoes significant increase with age as an effect of movie which might be leading to the misestimation of uncertainty.

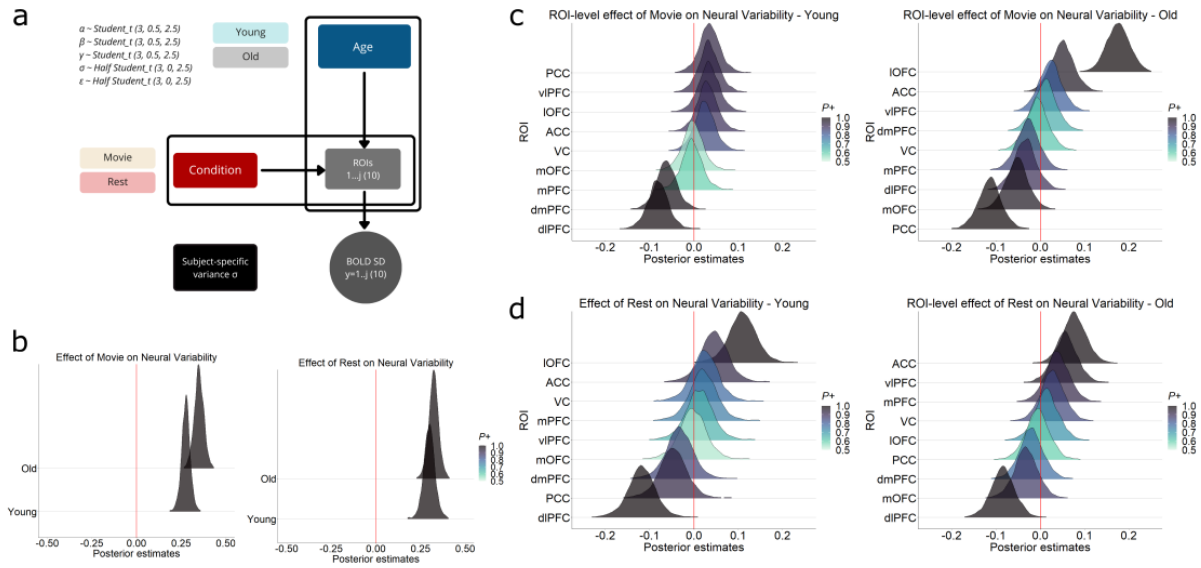

Figure 3: *(a) Graphical illustration of the BHR. Two predictors – Condition (categorically defined as movie or resting state) and Age (categorically defined as Young and Old) were used to analyse their interactive effect on the neural variability (SD_{BOLD}) of the ROIs. (b) Main effect of movie and rest on SD_{BOLD}. (left) Posterior density estimates shows significantly more evidence in old than young (P = 0.99, BF>100) in movie than that in rest (right) (P = 0.84, BF = 5.84). This suggests the SD_{BOLD} varies as a function of stimulus (movie) rather than being entirely structurally dependent. (c) ROI-level effect of the movie. (left) The movie significantly modulated the neural variability of the dmPFC and dlPFC and not any other prefrontal areas in young. (right) In case of old the effect of movie was found to significantly modulate the neural variability of only the lOFC among the prefrontal areas. (d) ROI-level effect of the rest. (left) The resting state significantly modulated the neural variability of the lOFC and dlPFC and not any other prefrontal areas in young. (right) In case of old the effect of rest was found to significantly modulate the neural variability of only the ACC and dlPFC.*

Distorted temporal latent state dynamics of the lOFC in old underlying neural variability

Our findings up till now revealed that older individuals exhibit a suboptimal computation of uncertainty, possibly linked to heightened neural variability in the lateral orbitofrontal cortex (lOFC). This increased variability might manifest as a distortion in the lOFC's representational dynamics of the movie

experience. That is, highly variable predictions in the lOFC might entail a highly unstable emotional experience. To explore the temporal latent state trajectory of the lOFC of the two groups, we performed a non-linear dimensional reduction method, T-PHATE on the BOLD timeseries of the lOFC. We found that the sequential temporal order of movie-watching is preserved in the young while it gets disrupted in the old (Fig. 4). Crucially, the consistency between neural data and behavioral ratings, despite originating from two distinct groups, underscores the impact of aging on emotional experiences. These findings shed light on how the lOFC's representation of temporal dynamics may be altered in older individuals, providing valuable insights into the interplay between neural variability and the affective uncertainty, ultimately shaping their emotional experiences.

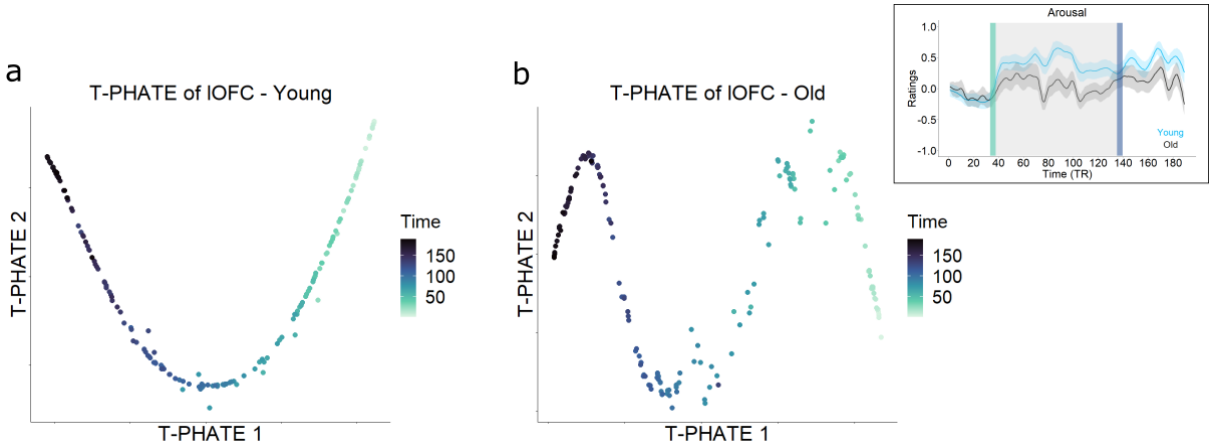

Figure 4: *Manifold embeddings of the lOFC using T-PHATE. Each data point is indexed by TR. (a) The latent temporal trajectory of the lOFC shows a conserved and sequential representation during a movie-watching task in young. (b) In contrast, the older adults exhibit a disrupted latent trajectory, indicating alterations in their temporal dynamics of the lOFC. Notably, the disrupted segments in their latent trajectory correspond to their differential emotional experiences during those specific parts of the movie (as can be seen from the arousal ratings in inset). Importantly, despite the neural and behavioral data being from two independent groups of participants, a similar pattern is observed in both.*

Discussion

The key advance of our work is to show how the variability around valence can explain a myriad of age-associated emotional responses, commonly thought of as idiosyncrasy. Aging alters the ability of the orbitofrontal cortex to represent emotions in a stable way, thereby having an increased uncertainty around the inferred valence which leads to distinct behavioural and neural phenomena. We found strong signatures of idiosyncratic responses within the older cohort in different emotional tasks, comprising of affect perception from facial expressions as well as discrete and continuous emotional responses while watching socially and emotionally charged videos. Interestingly, this variability is characterized by the

overlap of adjacent emotions, creating a suboptimal emotional response profile. A Bayesian learning model produced qualitative patterns of high uncertainty around valence and frequent updates to predictions of the valence, both of which mirrored the neural observations in the lOFC. These results as a whole advance our understanding of how aging alters our emotional experience, in a region known for uncertainty coding, within a single Bayesian brain framework, without the need for bespoke theories to explain disjunctive evidence (Mikels & Taullahu, 2023).

This facilitated us to investigate our main hypothesis of whether these variability can be attributed to the misestimation of uncertainty in older adults. This was also motivated by compelling evidence from decision-making literature which suggests that older adults have difficulty in dealing with uncertainty in learning under dynamic environment (Bruckner et al., 2020; Nassar et al., 2016). To identify the possible computational alterations in uncertainty estimation with age, we implemented multiple versions of a Bayesian learner model. Our generative modelling approach resonates with the central tenet of hierarchical processing of emotion dynamics under a Bayesian framework (Mathys et al., 2011), just like other higher-order cognitive phenomena (Siegel et al., 2018). Crucially, in our previous study, the normative variant of this Bayesian model provided valuable insights into how uncertainty can naturally arise within a hierarchically connected architecture, particularly in younger individuals (Majumdar et al., 2023). Here, we leveraged this architecture and selectively lesioned two free parameters mediating the computation of (posterior) uncertainty. We formalized our prediction on the misestimation of uncertainty in elderly individuals by putting forth several competing hypotheses regarding how the computation of uncertainty would affect the evolving beliefs about valence. The model output revealed three qualitatively distinct insights. First, the winning model showed considerably higher variance around the valence for the older adults. The suboptimal uncertainty estimation around predictions of the valence, might explain the variability of responses observed in all 3 emotional tasks in older cohort relative to young agnostic to the response profile issues such as purely motor/action-related variability.

Secondly, mapping to neural results, the highly uncertain predictions and repeated updates to it in the elderly individuals was manifested by the frequent latent state transitions in the lOFC, which had shown stable representations in the young. Similar unstable representation has been reported in older adults in learning under uncertainty in reversal tasks (Hämmerer et al., 2019). Our focus on the lOFC is strongly built on the extensive evidence from our previous study as well as its implication in normal emotion processing. Moreover, this is a region widely implicated in anxiety disorders which also

underlies a misestimation in the uncertainty (Pulcu & Browning, 2019). On a deeper look into the latent space, this coincided with disrupted temporal trajectories of experience in the old compared to a temporally preserved component observed in young. In this study, it remains unresolved whether these updates solely originate from wider beliefs about the evolving context, mental states of people in the stimuli or inferring one's own belief about them internally. This question may necessitate using different stimuli more amenable to control and experimentation.

Third, neural variability within this region in the older adults was higher than young brains, specific to the movie. What could be the underlying reason for this? There are many equally attractive propositions for neural variability from adaptation to noise, to Bayesian sampling where neuronal variability stems from uncertainty around the sampling distribution (Fiser & Lengyel, 2019). Even though the latter seems an attractive choice here, we make no strict commitment to any as this is generally an open question. The story of neural variability in healthy aging continues to gain momentum (Garrett et al., 2010, 2011) because of its potential to explain cognitive task performances, and its increasing role in being a predictor of age (Boylan et al., 2021; Garrett et al., 2013). In this study, we showed that the emotional idiosyncrasies in the older adults were reflected by increased neural variability in the lOFC, possibly due to its altered representation of uncertainty. Specifically, by comparing the effect of the movie and resting state on neural variability, we showed this cannot be explained solely by age-related structural changes. Apart from reinforcing the role of lOFC in affective tasks, this also reflects the domain-specific (emotion), region-specific (lOFC) and task-specific (movie) nature of this measure (BOLD variability) outlawing any simple directional hypothesis on this, free from the experimental setting. Thus, this misestimation of uncertainty in the elderly, which we observed at both computational and representational levels, interestingly established a link between the behavioral idiosyncrasy with that of the neural variability. Our modelling approach here of lesioning a computational model, is similar to ablation studies but stands in contrast to conventional cognitive model fitting methods and offers a valuable avenue for hypothesis testing in affective studies in datasets with rich naturalistic stimuli but lacking emotion ratings.

Cognitively demanding tasks such as working memory, episodic recall, or semantic control might require representing and navigating a higher dynamic range of states to perform optimally, and to represent them in a stable regime to be able to execute consistently. Emotions, however, are an exception since representing a wider gamut might actually be misleading (at best) or paralyzing (at worst). Indeed,

misestimation of uncertainty has been proposed to underlie many of common psychiatric disorders (Pulcu et al., 2022). The higher variability observed in the older cohorts seems to be consistent with the computational findings observed in our model as well as in studies investigating this in reward learning literature. Carefully put together, this suggests that a deviant uncertainty processing during hierarchical inference can explain a wide range of paradoxical observations in aging during emotion tasks and can be linked to prefrontal failure to represent uncertainty efficiently.

Theoretical frameworks such as neural sampling seems a highly plausible candidate for explaining the connection between neural and behavioral variability, however the gulf between electrophysiological studies/theoretical models of sampling and BOLD data still remains high, not the least with the grave differences in resolution imaged. Our findings also make a case for exploring circuit-level mechanisms within the OFC that may be specialized to uncertainty processing over long time-scales thus affecting emotions. Future studies can migrate to controlled stimuli with modulating uncertainty/variance levels in the stimuli and observe how this would affect neural variability (in the PFC), and more importantly in the behaviour in various forms of decision-making. Overall, here we contribute a strong piece of evidence of misrepresenting uncertainty, within a systematic framework of Bayesian brain perspective to explain the emotional differences originating in the aging brain. More nuanced questions on social contexts, positive emotions, network level dynamics remain – but we hope to have furnished a potential framework for answering them.

Materials and methods (1240)

Participants

We divided our participant pool into two groups – Young (18-35 years) and Old (60-88 years). After preprocessing, a total of 209 individuals (Young: N = 111, μ_{age} = 28.5±4.9, Male = 48; Old: N = 98, μ_{age} = 77±5, Male = 45) were selected from the healthy population derived Cambridge Centre for Aging and Neuroscience (CamCan) cohort for this study (Shafto et al., 2014). Owing to the absence of behavioral data of the neuroimaging participants for the movie stimulus, we additionally collected continuous ratings of 120 participants on an online platform (Prolific) (see SI Appendix).

Behavioral tasks and analysis

We explored the participants' responses to both discrete and dynamic stimuli by leveraging the FER and EmoR datasets from the CamCan repository as well as the continuous ratings of the online participants.

Facial Emotion Recognition task

Participants were presented with a series of emotional faces and for each trial, they had to characterize the emotion from six emotion categories – happy, sad, anger, fear, disgust, and surprise. To compare their differences in emotion perception we performed a one-sample *t*-test between the correct responses of the young and older individuals for each of the 6 categories. Next, to investigate potential misrepresentations of emotion, possibly stemming from increased valence variability, we generated cooccurrence matrices for the two groups across these 6 categories. Each point in the matrix represented the counts of responded emotions falling within the true emotion category, with diagonal elements set to 1 to signify instances where the responded emotion matched the true category. This was visualized as a chord diagram with a threshold of 1.6. Furthermore, we investigated the within-group and between-group behavioral variability (SD) across all categories and for each category respectively.

Emotional Reactivity and Regulation task

Participants viewed short video clips of 30 seconds, chosen from a wide range of videos categorized into Positive (e.g. Babies playing), Negative (e.g. Accident) or Neutral (e.g. Workplace demonstration) clips. The presentation of the video was preceded by a cue to watch or regulate. For our study, we only

selected the responses to the Watch condition, where participants were instructed to rate their emotional response on scales of 0 – 100 on how positive and negative they felt after each clip. Thereby, for each group, their behavioral ratings were classified into 6 types – Negative-watch-Negative (NegW_neg), Negative-watch-Positive (NegW_pos), Positive-watch-Negative (PosW_neg), Positive-watch-Positive (PosW_pos), Neutral-watch-Negative (NeuW_neg) and Neutral-watch-Positive (NeuW_pos). We compared the subjective ratings (positive and negative) and the between-group variability of their responses for each condition.

Continuous rating task

Our main behavioral and neuroimaging analyses were centered around a short, suspenseful movie called "Bang! You're dead" (8mins) by Alfred Hitchcock. Six independent groups of participants continuously rated the movie for valence, uncertainty, and arousal using a vertical slider on Prolific (see SI Appendix, Table S1). After rejecting subjects with missing data, this resulted in a final sample of 97 participants (Y: N = 50, μ_{age} = 24.5, Male = 23; O: N = 47, μ_{age} = 67.8, Male = 24). For each group, we z-scored the participants responses and smoothed the averaged time courses using local regression smoothing (loess).

fMRI acquisition and preprocessing

The fMRI data for the movie-watching and the resting state sessions were provided by the CamCan (Shafto et al., 2014). The functional scans for the movie-watching session were acquired using a T2∗-weighted echo planar imaging pulse sequence (TR = 2470 ms; TE = 9.4 ms, 21.2 ms,33 ms, 45 ms, 57 ms; 32 axial slices; slice thickness = 3.7 mm; FOV = 192 × 192 mm; voxel size = 3 × 3 × 4.44 mm), leading to a total of 193 volumes. The functional data for resting state was acquired using the same pulse sequence and acquisition parameters with a TR of 1970 ms. The acquisition time for this session was 8 min 40 s, which resulted in 261 functional volumes. The first 4 functional volumes of both sessions were discarded from the main analyses. Standard preprocessing pipeline was implemented for both sessions using SPM12 (see SI Appendix).

Behavioral modelling - Hierarchical Gaussian Filter (HGF)

To investigate the age-related changes in the computation of uncertainty during affective experience, we compared and contrasted multiple variants of the HGF (3-level) (Mathys et al., 2011) (see SI

Appendix). Our goal was to test a few competing hypotheses, especially, whether the older adults differed with regards to – 1) computation of variance around the fluctuating valence across the movie and 2) updating their belief trajectory in the face of changing uncertainty on the valence (Fig. 2a).

To formalize these predictions, we simulated multiple models manipulating 2 free parameters ω and ϑ (SI Appendix, Table S2), the tonic parameters for the second and third level respectively. An increase in ω would indicate a higher uncertainty estimate (at the 2nd level) on the changing valence, whereas its decrease would indicate vice-versa. Thus, both can result in the misestimation of uncertainty. The meta-volatility parameter ϑ, influences the belief updates on the volatility (3rd level) of the valence. The resultant belief trajectories were visually inspected and after considering the Log-Model Evidence (LME), we selected the best model which could offer a parsimonious explanation of the idiosyncratic response of the older people (more details SI Appendix).

Hidden Markov Model (HMM)

To explore whether the misestimation of uncertainty is reflected in the latent state representations of the lOFC, we fit an HMM to the individual subject's BOLD time series of lOFC and VC (for control) (see SI Appendix for ROI definition) for both groups, generating a single emission sequence across all participants of a group. Multiple models were created from prespecified states of range 2 to 10 which were then adjudicated by selecting the one with the least Bayesian information criteria (BIC). Parameter estimation for the models was done using the Baum-Welch algorithm (a variant of the Expectation-Maximization algorithm) by iteratively maximizing the expected joint log-likelihood of the parameters, given the observations and states. Decoding was done by the Viterbi algorithm by computing the maximum a posteriori state sequence for each of the HMMs.

Bayesian hierarchical regression (BHR)

Next, we investigated whether high volatility observed at the computational level is manifested as high neural variability in the elderly within the lOFC. For this we modelled the effect of rest and movie with age on the BOLD variability of the participants, using a BHR (Fig. 3a). The dependent variable for the model input was given by the SD_{BOLD} of 8 ROIs which included all prefrontal ROIs (mOFC, mPFC, dmPFC, lOFC, vlPFC, dlPFC, ACC) along with VC. The SD_{BOLD} of each session (Rest/Movie) for each subject was computed as the SD of the normalised, filtered and demeaned BOLD timeseries of each

ROI (See SI Appendix for more details). Significance levels, or evidence, were calculated by estimating the evidence of posterior probability.

Temporal Potential of Heat-diffusion for Affinity-based Transition Embedding (PHATE)

Finally, we sought to explore,whether the miscomputation of uncertainty, owing to the heightened neural variability is reflected at the low-dimensional temporal trajectory of the lOFC between the two groups. For this we implemented a non-linear, unsupervised dimensional-reduction technique called temporal PHATE (T-PHATE) (Busch et al., 2023). PHATE is recognized for its distinct advantages compared to conventional dimensional-reduction techniques like PCA and tSNE, as it effectively preserves both local and global data structures. Additionally, its non-linear nature and ability to capture the temporal evolution of a component present in the stimulus makes it well-suited for naturalistic paradigm (See SI Appendix).

Funding Information

NBRC Core funds supported this study. DR was supported by SERB Core Research Grant (CRG) S/SERB/DPR/20230033 extramural grant from the Department of Science and Technology, Ministry of Science and Technology, Govt. India. DR and AB acknowledge the generous support of the NBRC Flagship program BT/MIDI/NBRC/Flagship/Program/2019: Comparative mapping of common mental disorders (CMD) over the lifespan.

References

Atkinson, L., Murray, J. E., & Halberstadt, J. (2021). Older Adults' Emotion Recognition Ability Is Unaffected by Stereotype Threat. *Frontiers in Psychology*, *11*, 605724. https://doi.org/10.3389/FPSYG.2020.605724/BIBTEX

Boylan, M. A., Foster, C. M., Pongpipat, E. E., Webb, C. E., Rodrigue, K. M., & Kennedy, K. M. (2021). Greater BOLD Variability is Associated with Poorer Cognitive Function in an Adult Lifespan Sample. *Cerebral Cortex*, *31*(1), 562–574. https://doi.org/10.1093/cercor/bhaa243

Bruckner, R., Nassar, M. R., Li, S. C., Eppinger, B., & Carney, N. D. (2020). Default beliefs guide learning under uncertainty in children and older adults. *PsyArXiv*, 1–50.

Busch, E. L., Huang, J., Benz, A., Wallenstein, T., Lajoie, G., Wolf, G., Krishnaswamy, S., & Turk-Browne, N. B. (2023). Multi-view manifold learning of human brain-state trajectories. *Nature Computational Science 2023 3:3*, *3*(3), 240–253. https://doi.org/10.1038/s43588-023-00419-0

Campbell, K. L., Shafto, M. A., Wright, P., Tsvetanov, K. A., Geerligs, L., Cusack, R., Tyler, L. K., Brayne, C., Bullmore, E., Calder, A., Dalgleish, T., Duncan, J., Henson, R., Matthews, F., Marslen-Wilson, W., Rowe, J., Cheung, T., Davis, S., Kievit, R., … Villis, L. (2015). Idiosyncratic responding during movie-watching predicted by age differences in attentional control. *Neurobiology of Aging*, *36*(11), 3045–3055. https://doi.org/10.1016/j.neurobiolaging.2015.07.028

Chan, S. C. Y., Schuck, N. W., Lopatina, N., Schoenbaum, G., & Niv, Y. (2021). Orbitofrontal Cortex and Learning Predictions of State Transitions. *Behavioral Neuroscience*, *135*(4), 487–497. https://doi.org/10.1037/BNE0000461

Clark, A. (2013). Whatever next? Predictive brains, situated agents, and the future of cognitive science. The Behavioral and Brain Sciences, 36(3), 181–204. https://doi.org/10.1017/S0140525X12000477

Cortes, D. S., Tornberg, C., Bänziger, T., Elfenbein, H. A., Fischer, H., & Laukka, P. (2021). Effects of aging on emotion recognition from dynamic multimodal expressions and vocalizations. *Scientific Reports*, *11*(1), 1–12. https://doi.org/10.1038/s41598-021-82135-1

DC Knill, A. P. (2004). The Bayesian brain: the role of uncertainty in neural coding and computation. *Trends Neurosci.*, *27*(12), 712–719. https://doi.org/10.1016/j.tins.2004.10.007

Festa, D., Aschner, A., Davila, A., Kohn, A., & Coen-Cagli, R. (2021). Neuronal variability reflects probabilistic inference tuned to natural image statistics. Nature Communications 2021 12:1, 12(1), 1–11. https://doi.org/10.1038/s41467-021-23838-x

Fiser, J., & Lengyel, G. (2019). A common probabilistic framework for perceptual and statistical learning. *Current Opinion in Neurobiology*, *58*, 218–228. https://doi.org/10.1016/J.CONB.2019.09.007

Garrett, D. D., Kovacevic, N., McIntosh, A. R., & Grady, C. L. (2010). Blood oxygen level-dependent signal variability is more than just noise. *Journal of Neuroscience*, *30*(14), 4914–4921. https://doi.org/10.1523/JNEUROSCI.5166-09.2010

Garrett, D. D., Kovacevic, N., McIntosh, A. R., & Grady, C. L. (2011). The Importance of Being Variable. *Journal of Neuroscience*, *31*(12), 4496–4503. https://doi.org/10.1523/JNEUROSCI.5641-10.2011

Garrett, D. D., Kovacevic, N., McIntosh, A. R., & Grady, C. L. (2013). The Modulation of BOLD Variability between Cognitive States Varies by Age and Processing Speed. *Cerebral Cortex*, *23*(3), 684–693. https://doi.org/10.1093/CERCOR/BHS055

Grady, C. L., & Garrett, D. D. (2018). Brain signal variability is modulated as a function of internal and

external demand in younger and older adults. NeuroImage, 169, 510–523. https://doi.org/10.1016/J.NEUROIMAGE.2017.12.031

Hämmerer, D., Schwartenbeck, P., Gallagher, M., FitzGerald, T. H. B., Düzel, E., & Dolan, R. J. (2019). Older adults fail to form stable task representations during model-based reversal inference. *Neurobiology of Aging*, *74*, 90–100. https://doi.org/10.1016/j.neurobiolaging.2018.10.009

Hénaff, O. J., Boundy-Singer, Z. M., Meding, K., Ziemba, C. M., & Goris, R. L. T. (2020). Representation of visual uncertainty through neural gain variability. *Nature Communications 2020 11:1*, *11*(1), 1–12. https://doi.org/10.1038/s41467-020-15533-0

Hipólito, I., & Kirchhoff, M. (2023). Breaking boundaries: The Bayesian Brain Hypothesis for perception and prediction. *Consciousness and Cognition*, *111*, 103510. https://doi.org/10.1016/J.CONCOG.2023.103510

Katthagen, T., Fromm, S., Wieland, L., & Schlagenhauf, F. (2022). Models of dynamic belief updating in psychosis—a review across different computational approaches. *Frontiers in psychiatry*, *13*, 814111.

Majumdar, G., Yazin, F., Banerjee, A., & Roy, D. (2022). Emotion dynamics as hierarchical Bayesian inference in time. *Cerebral Cortex (New York, N.Y. : 1991)*. https://doi.org/10.1093/CERCOR/BHAC305

Mathys, C., Daunizeau, J., Friston, K. J., & Stephan, K. E. (2011). A Bayesian Foundation for Individual Learning Under Uncertainty. *Frontiers in Human Neuroscience*, *0*(MAY), 39. https://doi.org/10.3389/FNHUM.2011.00039

Mikels, J. A., & Taullahu, D. B. (2023). Emotion, Aging, and Decision Making: A State of the Art Mini-Review. *Advances in Geriatric Medicine and Research*, *5*(1). https://doi.org/10.20900/AGMR20230003

Nassar, M. R., Bruckner, R., Gold, J. I., Li, S.-C., Heekeren, H. R., & Eppinger, B. (2016). Age differences in learning emerge from an insufficient representation of uncertainty in older adults. *Nature Communications 2016 7:1*, *7*(1), 1–13. https://doi.org/10.1038/ncomms11609

Nogueira, R., Abolafia, J. M., Drugowitsch, J., Balaguer-Ballester, E., Sanchez-Vives, M. V., & Moreno-Bote, R. (2017). Lateral orbitofrontal cortex anticipates choices and integrates prior with current information. *Nature Communications 2017 8:1*, *8*(1), 1–13. https://doi.org/10.1038/ncomms14823

Posner, J., Russell, J. A., & Peterson, B. S. (2005). The circumplex model of affect: An integrative approach to affective neuroscience, cognitive development, and psychopathology. *Development and Psychopathology*, *17*(3), 715. https://doi.org/10.1017/S0954579405050340

Pulcu, E., & Browning, M. (2019). The Misestimation of Uncertainty in Affective Disorders. *Trends in Cognitive Sciences*, *23*(10), 865–875. https://doi.org/10.1016/J.TICS.2019.07.007

Pulcu, E., Saunders, K. E. A., Harmer, C. J., Harrison, P. J., Goodwin, G. M., Geddes, J. R., & Browning, M. (2022). Using a generative model of affect to characterize affective variability and its response to treatment in bipolar disorder. *Proceedings of the National Academy of Sciences of the United States of America*, *119*(28), e2202983119. https://doi.org/10.1073/PNAS.2202983119/SUPPL_FILE/PNAS.2202983119.SAPP.PDF

Reed, A. E., & Carstensen, L. L. (2012). The theory behind the age-related positivity effect. *Frontiers in Psychology*, *3*(SEP), 30180. https://doi.org/10.3389/FPSYG.2012.00339/BIBTEX

Schweizer, S., Stretton, J., van Belle, J., Price, D., Calder, A. J., & Dalgleish, T. (2019). Age-related decline

in positive emotional reactivity and emotion regulation in a population-derived cohort. *Social Cognitive and Affective Neuroscience*, *14*(6), 623–631. https://doi.org/10.1093/scan/nsz036

Schuck, N. W., Doeller, C. F., Polk, T. A., Lindenberger, U., & Li, S. C. (2015). Human aging alters the neural computation and representation of space. *NeuroImage*, *117*, 141–150. https://doi.org/10.1016/j.neuroimage.2015.05.031

Shafto, M. A., Tyler, L. K., Dixon, M., Taylor, J. R., Rowe, J. B., Cusack, R., Calder, A. J., Marslen-Wilson, W. D., Duncan, J., Dalgleish, T., Henson, R. N., Brayne, C., & Matthews, F. E. (2014). The Cambridge Centre for Ageing and Neuroscience (Cam-CAN) study protocol: a cross-sectional, lifespan, multidisciplinary examination of healthy cognitive ageing. *BMC Neurology 2014 14:1*, *14*(1), 1–25. https://doi.org/10.1186/S12883-014-0204-1

Siegel, J. Z., Mathys, C., Rutledge, R. B., & Crockett, M. J. (2018). Beliefs about bad people are volatile. *Nature Human Behaviour 2018 2:10*, *2*(10), 750–756. https://doi.org/10.1038/s41562-018-0425-1

Sze, Jocelyn A., Madeleine S. Goodkind, Anett Gyurak, and Robert W. Levenson. "Aging and emotion recognition: not just a losing matter." *Psychology and aging* 27, no. 4 (2012): 940.

Taylor, J. R., Williams, N., Cusack, R., Auer, T., Shafto, M. A., Dixon, M., Tyler, L. K., Cam-CAN, & Henson, R. N. (2017). The Cambridge Centre for Ageing and Neuroscience (Cam-CAN) data repository: Structural and functional MRI, MEG, and cognitive data from a cross-sectional adult lifespan sample. *NeuroImage*, *144*, 262–269. https://doi.org/10.1016/J.NEUROIMAGE.2015.09.018

Tobler, P. N., O'Doherty, J. P., Dolan, R. J., & Schultz, W. (2007). Reward Value Coding Distinct From Risk Attitude-Related Uncertainty Coding in Human Reward Systems. *Journal of Neurophysiology*, *97*(2), 1621. https://doi.org/10.1152/JN.00745.2006

Visser, M. (2020). Emotion Recognition and Aging. Comparing a Labeling Task With a Categorization Task Using Facial Representations. *Frontiers in Psychology*, *11*(February), 1–7. https://doi.org/10.3389/fpsyg.2020.00139

S.I. Appendix

Participants

We extracted the behavioral responses of the same CamCan participants for the Facial Emotion Recognition (FER) and Emotional Reactivity and Regulation (EmoR) tasks. Owing to missing data, the final sample size for the FER was 203 (Y = 108, O = 95), and that of EmoR was 91 (Y = 49, μ_{age} = 28±5; O = 42, μ_{age} = 76.9±5.7). All participants provided their informed consent, and the data was collected in accordance with the Cambridgeshire Research Ethics Committee.

Additionally, we recruited independent groups of participants on an online platform (Prolific) to collect continuous ratings for arousal, valence, and uncertainty for the same movie shown to the neuroimaging participants. 60 participants were recruited for each age group and demographically matched with the fMRI individuals (UK). All participants were screened based on educational qualification and mental health status to reduce potential confounds, and no previous history of watching this movie was reported. The Institutional Human Ethics Committee of the National Brain Research Centre, India (NBRC) approved the study.

fMRI preprocessing

Neuroimaging data from both sessions were preprocessed in MATLAB (2019b) using Statistical Parametric Mapping (SPM12) (https://www.fil.ion.ucl.ac.uk/spm). The preprocessing steps included spatial realignment, slice-timing correction, coregistration of functional (T2) to anatomical (T1) scans, affine transformation to Montreal Neurological Institute template (MNI152), resampling to 2 mm isotropic voxels, and spatial smoothing with a 6 × 6 × 9-mm full-width at half-maximum Gaussian kernel. Whole-movie GLM (SI Appendix) was computed by regressing six motion parameters (X-, Y-, Z-displacement and pitch, roll, and yaw parameters) by least square regression. We excluded subjects with maximum framewise displacement >2.5 mm or 1.5° from further analysis. The extracted BOLD data were detrended and band-pass filtered (0.01–0.1 Hz) using a second-order Butterworth filter.

Region-of-interest (ROI) definition

Given compelling evidence from the literature and our previous study suggesting a central role of lOFC in representing subjective uncertainty and mediating emotional experience during movie-watching tasks, we focused our analyses primarily on the lateral orbitofrontal cortex (lOFC). For the neural variability analyses

of the movie and resting state, we included 6 additional prefrontal ROIs – anterior cingulate cortex (ACC), dorsolateral PFC (dlPFC), dorsomedial (dmPFC), ventrolateral PFC (vlPFC), medial PFC (mPFC) and medial orbitofrontal cortex (mOFC). We also incorporated the visual cortex (VC) as a control ROI. All ROI masks were adapted from our previous work, where additional details can be found (Majumdar et al., 2023).

Hierarchical Gaussian filter (HGF) model

The hierarchical Gaussian filter (HGF) is a Bayesian learning model (Mathys et al., 2011)that can fit and recover parameters from a participant's behavioral data or simulate models with different parameter configurations, scored on Log Model Evidence (LME). In brief, by employing variational Bayes, this model can infer an individual's belief and uncertainty trajectory of hidden environmental states, modeled as a hierarchy of coupled Gaussian random walks. Since we did not have any behavioral response from the neuroimaging participants, we only used a perceptual model on a Bayes-optimal agent with the average valence ratings of each group as the input using the TAPAS toolbox (http://www.translationalneuromodeling.org/tapas/).

The HGF is commonly implemented to model learning under uncertainty dynamically. However, this model previously enabled us to uncover a predictive architecture where volatility trajectory estimated from the valence ratings reflected the subjective uncertainty of the participants (Majumdar et al., 2023) during affective experiences. In this study, we aimed to test a few competing hypotheses regarding the computational changes in older people underlying their idiosyncratic behavior in affective tasks relative to younger participants. Thus, this can be construed as a model 'lesioning' wherein a normative model that explains a behavioral quantity and its latent parameters are altered such that qualitative predictions similar to the data can be assessed. For this, we simulated multiple variants of the HGF (3-level).

Since we used the averaged valence trajectory as input for each group, the first layer, x_1, models the probability of the valence at each time point. The next level, x_2, estimates the underlying uncertainty associated with the predictions on the valence. Finally, the third level, x3, estimates the overall volatility associated with the valence, i.e., the rate at which the belief in the uncertainty around valence changes. These levels are related to each other with regard to the step-size of a Gaussian random walk. A prediction error, i.e., a misestimation of the valence at the lower level, will cause an update at the higher levels. These

levels are coupled to each other by parameter $\boldsymbol{\kappa}$, which denotes a phasic, temporally varying parameter that determines the scaling of the volatility. Since we had no specific hypotheses on how this coupling might change with age, we kept the $\boldsymbol{\kappa}$ same for both groups. Our main hypotheses rested with the $\boldsymbol{\omega}$ and $\boldsymbol{\vartheta}$ parameters that denote a tonic, time-invariant parameter for the second and third levels, respectively. $\boldsymbol{\Omega}$ captures the degree to which an agent updates his belief about the rate of change of valence $x_2^{(k)}$ independent of the volatility, and $\boldsymbol{\vartheta}$ determines meta-volatility or the variance of the agent's volatility. To analyze the effect of ω on the variance of belief around the changing valence, we compared the variance of the x_2 trajectories of both groups. Furthermore, we also compared how the $\boldsymbol{\omega}$ affected the belief updates in these two groups by binarizing their update trajectories (ud2) with a threshold of 1 SD.

Bayesian Hierarchical Regression to model the effect of uncertainty and valence on the neural activity

For this analysis, we defined 5 Ascent (high-intensity scenes marked by positive arousal slopes), 5 Descent (low-intensity scenes marked by negative arousal slopes), and 1 Control (neutral scene) segments from the arousal ratings of the young in a data-driven way. Here, we employed a Bayesian hierarchical regression model to delineate the age-associated effects of uncertainty and valence on emotion dynamics (Fig. S2a). The dependent measure of the model input was given by the % BOLD signal for each of the 8 ROIs (mentioned in the ROI definition) for each group relative to Control and was modeled as a Student *t*-distribution:

PSC = Student $t\,(v, \mu, \sigma)$,

where v is the degrees of freedom, σ is the scale parameter of the distribution, and μ is the mean which can be expressed as:

$\mu = \alpha + \alpha_j + \alpha_i + \beta_1$.Age + β_2.Uncertainty + β_3.Valence + β_4. Age: Uncertainty

+ β_5.Age : Valence

+ γ_{1j} Age | ROI

+γ_{2j}. Uncertainty | ROI

+γ_{3j}. Valence | ROI

+γ_{4j}. Age : Uncertainty | ROI

+γ_{5j}. Age : Valence | ROI

+γ_{6j}. Age | Subject

$+\gamma_{7j}$. Uncertainty | Subject

$+ \gamma_{8j}$. Valence | Subject + $\sigma_i + \varepsilon$.

Here, α is the intercept, α_j is the varying intercept over *j* ROIs, α_i is the varying intercept over *i* participants. β and γ reflect the slope and varying slope of the predictors, respectively. β_1 represents the slope for the age parameter (which was defined as a categorical variable -Y and O), β_2 and β_3 denote the slope for the Uncertainty and Valence, respectively. β_4 and β_5 denote the slope for the cross-level interaction term of age with valence and uncertainty, respectively. γ_{1j}, γ_{2j}, and γ_{3j} are varying slopes where each of the 3 predictors is allowed to vary across all *j* ROIs. γ_{4j} and γ_{5j} are varying slopes for the cross-level interaction terms of age with uncertainty and valence, allowed to vary across the ROIs. γ_{6i}, γ_{7i}, and γ_{8i} are varying slopes where each of the 3 predictors is allowed to vary across all *i* (=209) participants. The way we constructed the model enabled us to consider the effect of uncertainty and valence for the two conditions (we only show the Ascent here) across age and ROIs. Since the classification of scenes is based on the behavioral ratings of the young adults, we considered the entire movie for the main study. Here, we showed only the main effect of uncertainty and valence across age in modulating the neural activity.

Engagement analysis with whole-brain temporal intersubject correlation (ISC)

To determine whether engagement in older adults varies as a function of the emotional content of the stimulus, we performed an engagement analysis. For each condition (Ascent, Descent, and Control), we computed the whole brain temporal ISC of the older adults to compare their neural engagement with that of the Young and how it differed with the conditions. Each subject's whole-brain BOLD signal was extracted using the Power Atlas with 264 cortical and subcortical ROIs (Fig. S3).

Bayesian Hierarchical Regression to model the effect of movie and resting state on neural variability

To model the effect of rest and movie with age on the BOLD variability of the participants, we constructed this BHR. The SD_{BOLD} of each session (Rest/Movie) for each subject was modeled as a Student *t*-distribution:

SD_{BOLD} = Student $t\ (v, \mu, \sigma)$,

Where v is the degrees of freedom, σ is the scale parameter of the distribution, and μ is the mean, which can be expressed as:

$\mu = \alpha + \alpha_j + \alpha_i + \beta_1.\text{Age} + \beta_2.\text{Condition} + \beta_3.\text{Age: Condition}$

$+ \gamma_{1j}.$ Age | ROI

$+ \gamma_{2j}.$ Condition | ROI

$+ \gamma_{3j}.$ Age : Condition | ROI

$+ \gamma_{4i}.$ Age | Subject

$+ \gamma_{5i}.$ Condition | Subject $+ \sigma_i + \varepsilon$.

Here, α is the intercept, α_j is the varying intercept over j ROIs, and α_i is the varying intercept over i participants. β and γ reflect the slope and varying slope of the predictors, respectively. β_1 represents the slope for the age (given as a categorical variable), β_2 denotes the slope for the conditions (given as categorical variables - Rest and Movie), and β_3 denotes the slope for the cross-level interaction term of age and condition. γ_{1j} and γ_{2j} indicate the varying slope terms where the age and conditions vary across all the ROIs. γ_{3j} indicates the varying slope term where the cross-level interaction term (age and condition) varies across all the ROIs. Likewise, γ_{4i} and γ5i are varying slopes where the 2 predictors can vary across all I (=209) participants. σ_i and ε connote subject-level and population-level variance terms, respectively. Weak, noninformative priors were applied over the model terms. The model incorporated the effect of rest and movies as their interaction with age (categorically defined as Young and Old) while accounting for within-group and between-group variability on ROIs.

$\alpha \sim$ Student $t(3, 0.5, 2.5)$

$\beta \sim$ Student $t(3, 0.5, 2.5)$

$\gamma \sim$ Student $t(3, 0.5, 2.5)$

$\sigma_j \sim$ Half Student $t(3, 0, 2.5)$

$\varepsilon \sim$ Half Student $t(3, 0, 2.5)$

Evidence of P > 95% is equivalent to the frequentist depiction of significant P-values. In addition, we quantified the effect size by computing the BF (calculated by the Savage-Dickey ratio).

T-PHATE

We implemented the temporal PHATE to uncover the manifold embeddings of the lOFC for the two groups during the movie-watching task. It considers an input matrix of TR x Voxel, on which it computes the Euclidean distance D between two TRs, where D(i, j) = $||X_i, - X_j,||^2$. Then, it converts this matrix into a local affinity matrix K using an adaptive bandwidth Gaussian kernel. The affinity matrix K is then row-normalized to get the initial probabilities P, which are used for the Markovian random-walk diffusion process. The diffusion operator P is then raised to the t_Dth power, where t_D is the PHATE optimal diffusion time scale, to perform a t_D-step random walk over the data. This specific diffusion process effectively infers more global relations beyond the local affinities. To further preserve the local and manifold-intrinsic global data structure, PHATE computes the diffusion potential distance P_D between the distribution at the *i*th row $P^{tD}{}_i$ and at the *j*th row $P^{tD}{}_j$.

$$P_D(i,j) = \sqrt{\sum_k \left(\log\left(P^{t_D}(i,k) - P^{t_D}(j,k)\right)\right)^2}$$

The potential distance is finally embedded with a distance embedding method (multidimensional scaling—MDS) for final visualisation. This embedding accurately visualizes trajectories and data distances without requiring strict assumptions typically used by path-finding and tree-fitting algorithms. T-PHATE is a modified PHATE algorithm that can capture the temporal aspect of the data. The algorithm works the same as the original PHATE except for the temporal component infused in the diffusion matrix using the auto-covariance function in a Temporal Affinity Matrix (Busch et al., 2023).

Arousal: Click the white button (and hold it throughout) and drag it up or down depending on the intensity of emotion you feel while watching the movie, irrespective of whether you feel a positive or negative emotion.
Valence: Click the white button (and hold it throughout) and drag it up or down depending on whether you feel – positive (up) or negative (down). If it gets increasingly negative, you drag it further down from the centre and vice versa.
Uncertainty: Click the white button (and hold it throughout) and drag it up or down depending on how much uncertainty you feel at any given moment. In this movie, there will be certain events which might lead to positive or negative outcomes. Drag the scale up or down depending on how uncertain you feel about the ensuing outcome.

Table S1: Instructions for the continuous rating task conducted in Prolific. Participants had to continuously rate the movie on either of the 3 parameters by moving a vertical slider (encoded with values from -1 to +1) up and down while watching the movie.

	M1	**M2**	**M3**	**M4**	**M5**	**M6**	**M7**
$\omega_1\ \mu$	99993	99993	99993	99993	99993	99993	99993
$\boldsymbol{\omega_2\ \mu}$	-8	-4	-10	-4	-10	-4	-4
$\omega_1\ \sigma$	1	1	1	1	1	1	1
$\omega_2\ \sigma$	0.05	0.05	0.05	0.05	0.05	0.05	0.05
$\boldsymbol{\vartheta\ \mu}$	2	2	2	4	0	0.05	2
$\vartheta\ \sigma$	0.05	0.05	0.05	0.05	0.05	0.05	0.05
LME	1703	1553	1669	1717	1678	**1737**	1553

Table S2: Prior parameters for all simulated HGF models. Model adjudication was done by selecting the one with the highest Log Model Evidence (LME) (M6). The $\omega_2\mu$ and $\vartheta\mu$ parameters were iterated for each model, motivated by our specific hypothesis.

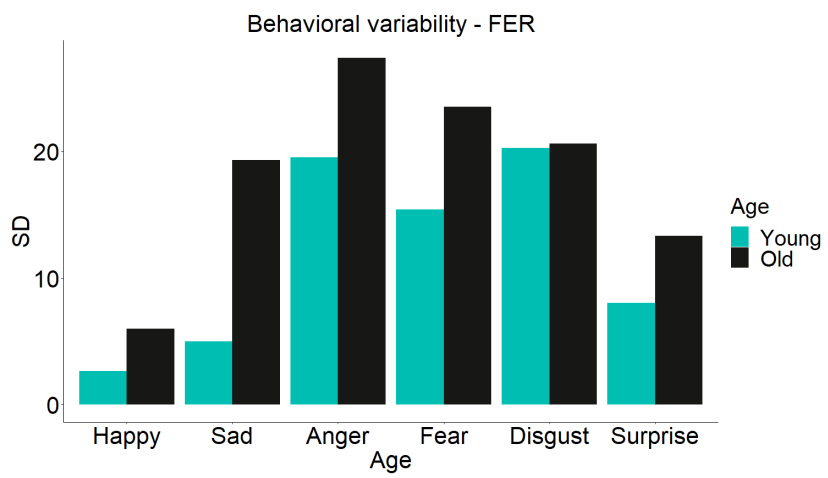

Figure S1: Between-group Variability in Participant Responses for Each Emotion Category illustrates the between-group variability of participants' responses in the Facial Expression Recognition (FER) task across the six emotion categories. All emotion categories show increased variability in older adults compared to younger individuals.

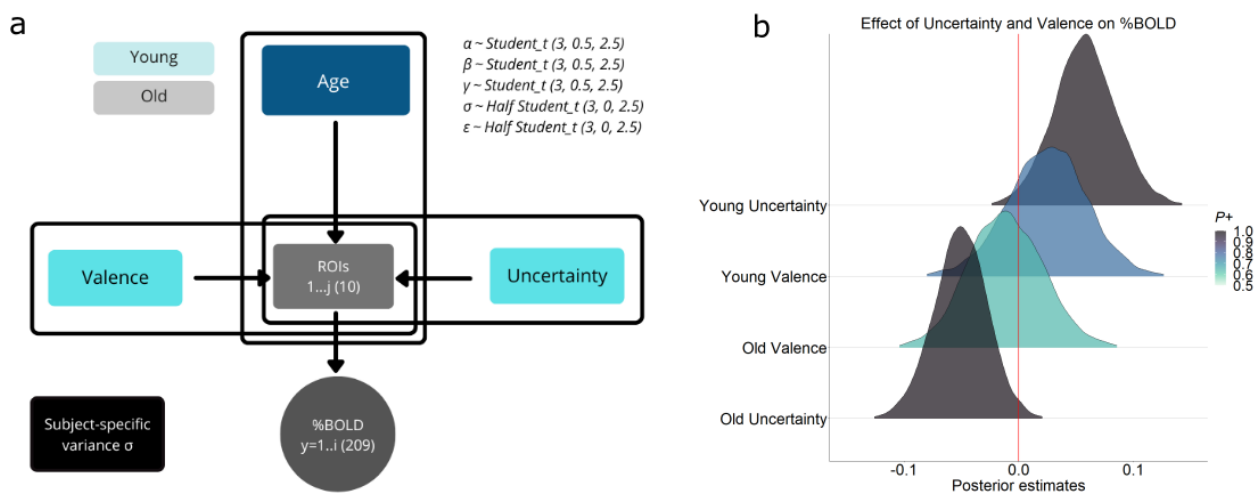

Figure S2: (a) Graphical illustration represents the architecture of the Hierarchical Bayesian model. BOLD % signal change was modeled to be drawn from a Student *t*-distribution and varied across groups, participants, and ROIs. Main effects of interest were the age-associated effect (categorically defined as Young and old) with the interaction terms of arousal (categorical predictor) with each of uncertainty and valence (as continuous predictors). (b) The main effect of Valence and Uncertainty in modulating the neural activity between the two groups. Posterior density estimates showing the effect of uncertainty significantly differ (Young: P = 0.98; Old: P= 0.98) between the two groups compared to the valence (Young: P = 0.77; Old: P = 0.64).

A potential point of critique may pertain to the stimulus classification, which is based on the ratings provided by the young participants. We refrained from scene categorization in our main analyses to address this concern and incorporated the entire movie series for behavioral and neural inferences.

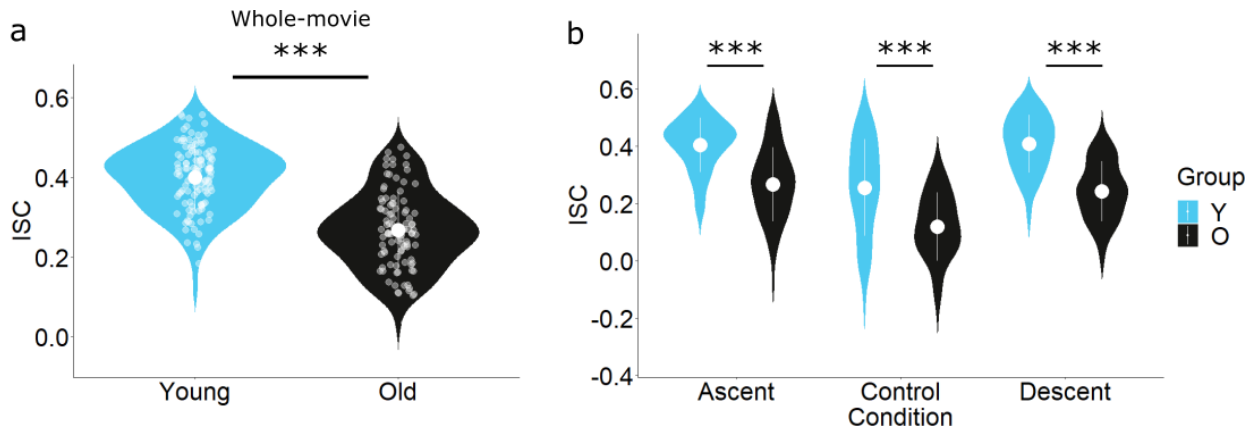

Figure S3: Shared neural engagement of Ascent, Descent, and Control computed from the whole-brain ISC of the two groups. If attentional processes were the main modulators of the neural activity in the old, we would expect a lower ISC in older adults affected similarly for all 3 conditions, irrespective of the emotional saliency of the scenes. Whole brain temporal ISC (whole brain parcellation by Power Atlas, 264 ROIs) on the movie-watching data for both groups (Y = 111; O = 98) revealed that (a) although the older individuals had lower ISC than Young for the entire movie (Young: r = 0.40; Old: r = 0.27; P < 0.0001) as well as (b) for all conditions (Ascent: Y – r = 0.41, O – r = 0.27, P < 0.0001; Descent: Y – r = 0.41, O – r = 0.24, P < 0.0001; Control: Y – r = 0.26, O – r = 0.12, P < 0.0001), within-group ISC of the old were higher for the Ascent and Descent compared to Control (similar pattern as Young). This suggests that the decreased neural engagement in the elderly varied as a function of the emotional saliency of the conditions.

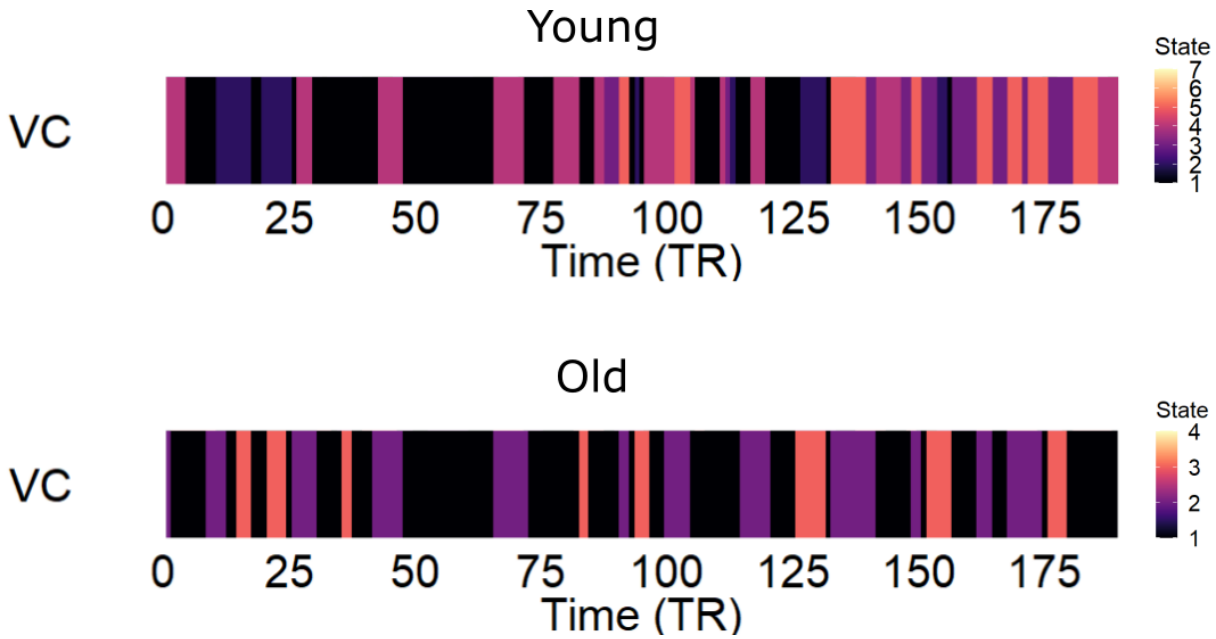

Figure S4: Comparison of the HMM state transitions of the Visual Cortex (VC) between the two groups showed faster transitions in both. This might reflect that sensory uncertainty processing (changing of visual features) is similar in both groups and cannot be attributed to the misestimation of higher-order uncertainty in the elderly.